



## EFFECT OF COPPER ON THE STRUCTURE AND OTHER PHYSICAL PROPERTIES OF CU-AS-TE CHALCOGENIDE GLASSES

N. ZOTOV<sup>a,\*</sup>, F. BELLIDO<sup>a</sup>, M. DOMINGUEZ<sup>a</sup>, R. JIMENEZ-GARAY<sup>a</sup>, A.C. HANNON<sup>b</sup>  
and R. SONNTAG<sup>c</sup>

<sup>a</sup>Facultad de Ciencias, Universidad de Cadiz, 11510 Puerto Real (Cadiz), Spain

<sup>b</sup>ISIS Facility, Rutherford Appleton Laboratory, Chilton, Didcot OX11 0QX, UK

<sup>c</sup>Hahn-Meitner Institut — BENSC, Glienicke str. 100, D-14109 Berlin, Germany

(Received 28 May 1996; accepted 16 December 1996)

**Abstract**—The first neutron diffraction radial distribution functions (RDF) of ternary Cu-As-Te chalcogenide glasses with general formula  $\text{Cu}_x\text{As}_{0.45-x}\text{Te}_{0.55}$  are presented. The average coordination numbers, derived from the area under the first RDF peak, indicate that there is a critical composition  $x_c \approx 0.06$ , below which the incorporation of copper does not practically change the Te coordination. Above this value the Te coordination starts to increase linearly from 2 to 4 with increasing  $x$ . This behaviour is confirmed by the compositional dependence of the mass density. A linear correlation,  $T_g(\text{K}) = 371 + 15.5 \text{ CN}$ , between the average coordination number CN, commonly associated with the rigidity of the network, and the glass transition temperature  $T_g$  is established, which indicates that the thermal stability of the glasses increases with increasing copper content. © 1997 Elsevier Science Ltd. All rights reserved

**Keywords:** chalcogenide glasses, neutron diffraction, structure, glass transition, density

### 1. INTRODUCTION

Ternary Cu-As-Te glasses are formed in a narrow compositional range adjacent to the binary  $\text{As}_{0.50}\text{Te}_{0.50}$  composition which is elongated in the direction of the Cu-Te tie line in such a way that above 55 atm.% Te glasses are formed only when the copper content exceeds 10–15 atm.% [1]. The glass formation region in the Cu-As-Se system is very similar to that for Cu-As-Te [1]. However, while the Cu-As-Se glasses with composition  $\text{Cu}_x\text{As}_{0.50-x}\text{Se}_{0.50}$ , where  $0.05 < x < 0.20$ , exhibit a strong first sharp diffraction peak (FSDP), the intensity of which decreases with increasing  $x$  [2], the existing diffraction data on Cu-As-Te glasses with similar compositions do not indicate the presence of FSDP [3–6]. The FSDP is commonly regarded as a signature of the medium-range order [7, 8] and therefore the substitution of Te for Se seems to introduce significant changes in the structure of these chalcogenide glasses. Besides that, while Cu-As-Se is one of the most studied systems by X-ray diffraction [9–11], extended X-ray absorption fine structure (EXAFS) spectroscopy [12–14], Nuclear Quadrupole Resonance (NQR) spectroscopy [15] and neutron diffraction [16], structural data for the Cu-As-Te glasses are very scarce.

The local structure and the crystallization of binary  $\text{As}_{1-y}\text{Te}_y$  glasses, where  $0.35 < y < 0.80$ , were reported in the comprehensive study of Corner and Rossier [17] and latter by Feigel *et al.* [18]. Electron diffraction radial

distribution functions (RDF) of amorphous  $\text{As}_2\text{Te}_3$  thin films has been published in Ref. [19] (and older references therein). The structure of several ternary  $\text{Cu}_x\text{As}_{0.5-x}\text{Te}_{0.5}$  chalcogenide glasses, where  $x = 0.05, 0.10, 0.15, 0.20$  and  $0.25$ , was studied by X-ray diffraction and structural models, consistent with the experimental X-ray RDFs, were constructed using the Metropolis Monte Carlo algorithm [3–6]. However, the number of atoms in these simulations (typically 100–150 atoms) was relatively small for statistical analysis of the bond length and bond angle distributions and especially for the investigation of the medium-range order in the Cu-As-Te glasses.

Therefore, we have decided to reexamine the structure of the Cu-As-Te glasses using both neutron and X-ray diffraction in order to take advantage of the different atomic scattering cross-sections of X-rays and neutrons. In the present paper we report the results from the first neutron diffraction experiments on Cu-As-Te glasses and compare them with density and glass transition temperature measurements. The neutron diffraction results together with new X-ray diffraction measurements (in progress) will be used later in combined Reverse Monte Carlo [20] simulations in order to produce realistic three-dimensional models of the structure and analyse in detail the medium-range order.

### 2. EXPERIMENTAL

#### 2.1. Sample preparation and characterization

Four Cu-As-Te glasses with general formula

\*To whom correspondence should be addressed.

$\text{Cu}_x\text{As}_{0.45-x}\text{Te}_{0.55}$  were prepared for the present study. Pure copper (99.999% Aldrich), arsenic (99.9999% Aldrich) and tellurium (99.9999% Aldrich) powders were ground in an agate mortar, sieved through a 45  $\mu\text{m}$  mesh and mixed together to obtain about 9 g of the corresponding composition. For each sample the powder was put into a quartz tube of 6 mm inner diameter and repeatedly evacuated–refilled with He. The tube was then sealed with an oxyacetylene burner while the residual gas pressure was about  $810^{-2}$  Torr. The ampoules were kept at 900°C for 24 h in a furnace and then quenched in ice water. In order to obtain good homogeneity of the samples, the ampoules were rotating at about 12 rpm. The composition of the final glassy alloys was determined using a Jeol JSM 820 SEM with EDAX X-ray dispersive analyser. The glass transition temperatures ( $T_g$ ) were measured by a Perkin Elmer DSC 7 thermal analyser. The samples consisted of about 20 mg powder in crimped (but not hermetically sealed) Al sample pans. All measurements were carried out in a dynamic atmosphere of dry  $\text{N}_2$  gas at a heating rate 10 K/min referenced to an empty Al pan. The density of each sample was measured pycnometrically five times in distilled water and the results averaged.

## 2.2. Neutron diffraction experiments

The samples with high copper content ( $x = 0.15$  and  $x = 0.20$ ) were measured at the neutron spallation source ISIS, UK. The samples with low copper content ( $x = 0.05$  and  $x = 0.10$ ) were measured at the neutron reactor BENSC, Berlin, Germany.

**2.2.1. ISIS experiments.** The diffraction measurements were performed using the LAD time-of-flight diffractometer, operating on the methane moderator. The powder samples (about 7 g) were loaded in cylindrical vanadium cans with inner radius 3.885 mm and wall thickness 0.085 mm. Data was collected by 88 detectors grouped into seven banks of detectors at mean  $2\theta$  values of 4.937, 9.704, 20.562, 35.183, 58.103, 90.131 and 148.164°, respectively. Diffraction patterns were taken for: (i) the two samples; (ii) the empty vanadium can; (iii) the instrumental background and (iv) a vanadium rod with 8.34 mm diameter. The samples were measured for about 20 h, the V can and the V rod for about 8 h.

The analysis of the data was made using the ATLAS suite of programs [21]. The data was first corrected for time-independent background. Then, the intensity for each group of detectors was rebinned from time-of-flight to  $Q$  units ( $Q = 4\pi\sin(\theta)/\lambda$ ) with spacing  $\Delta Q = 0.02 \text{ \AA}^{-1}$  and normalized by the incident monitor count. The data for each group of detectors were then corrected for instrumental background, placed on an absolute scale by dividing by the vanadium counts, corrected for multiple scattering and absorption in the sample plus can to obtain the differential cross-sections for all groups of detectors.

The self-scattering term,  $i_{\text{self}}(Q)$ , was then subtracted to obtain the distinct scattering curves,  $i(Q)$ . The  $i(Q)$  curves for all groups of detectors were then combined in the  $Q$  range from  $0.5 \text{ \AA}^{-1}$  to  $23 \text{ \AA}^{-1}$  to give the total distinct scattering curve for each sample. Finally the low- $Q$  part of the  $i(Q)$  curves was extrapolated to  $Q = 0.0$ .

**2.2.2. BENSC experiments.** The diffraction measurements were performed at the E2 flat-cone diffractometer [22], equipped with a position sensitive detector (PSD) covering  $80^\circ 2\theta$  and radial collimator, using a Cu(200) monochromator. The powder samples were loaded in cylindrical vanadium cans with inner radius 3.9 mm, wall thickness 0.1 mm, 50 mm height (40 mm in the beam). Diffraction patterns were taken for: (i) the two samples; (ii) the empty vanadium can; (iii) the instrumental background; (iv) vanadium rod with  $8.25 \pm 0.05$  mm diameter; and (v)  $\alpha$ -Fe powder standard. The diffraction patterns (except for the Fe standard and the instrumental background) were measured five times relative to an incident beam monitor from  $7$  to  $87^\circ 2\theta$  and from  $27$  to  $107^\circ 2\theta$ .

The intensities for each measurement were first corrected for the different efficiency of the channels of the PSD. At this step it was necessary to exclude the first 10 and the last 20 channels due to their anomalously high intensity. The data from the five measurements were then averaged, the background was subtracted and the averaged data was Fourier smoothed. The data from the two ranges were then scaled and merged together to give the final scattering curve for each sample, the V can and the V rod. The actual wavelength and the zero shift of the diffractometer were determined from refinements of the  $\alpha$ -Fe pattern using the Rietveld method [23]. The wavelength determined,  $\lambda = 0.916 \pm 0.005 \text{ \AA}$ , was used in the subsequent analysis.

The data were then corrected for multiple scattering using the method of Blech and Averbach [24]. Corrections for absorption in the sample and the can were then applied using the algorithms of Paalman and Pings [25]. The scattering and the absorption cross-sections of the samples, necessary for the multiple and absorption corrections, were calculated for  $\lambda = 0.916 \text{ \AA}$  using the data published by Sears [26] and the measured packing densities. The corrected data  $I(Q)$  were placed on an absolute scale by dividing with the V rod counts.

The distinct scattering,  $i(Q)$ , for each sample was then calculated by subtracting the  $i_{\text{self}}(Q)$  term from  $I(Q)$ . In this case  $i_{\text{self}}(Q)$  was calculated as

$$i_{\text{self}}(Q) = \sum b_j^2 (1 + P_j(Q))$$

where  $b_j$  is the isotopically averaged coherent scattering length and  $P_j(Q)$  is the inelasticity Placzek correction for nucleus  $j$  and the summation is over all atoms in the structural unit. The  $P_j(Q)$  terms were calculated according to Ref. [27] assuming that the detector efficiency for

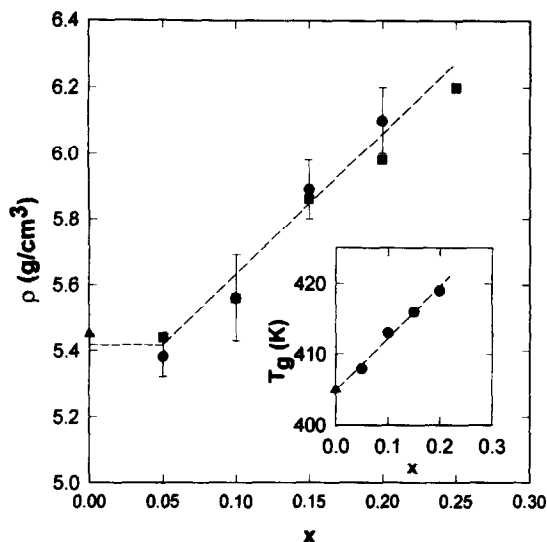


Fig. 1. Dependence of the bulk density of Cu-As-Te chalcogenide glasses on the copper content  $x$ : ( $\blacktriangle$ ) Borissova [1], ( $\bullet$ )  $\text{Cu}_x\text{As}_{0.45-x}\text{Te}_{0.55}$ -present study, ( $\blacksquare$ )  $\text{Cu}_x\text{As}_{0.50-x}\text{Te}_{0.50}$  [3–6]. The inset shows the dependence of the glass transition temperature  $T_g$  on  $x$ . The dashed lines are only guide for the eyes.

neutrons with wavelength  $\lambda = 0.91 \text{ \AA}$  is 24% and approximating further the mean kinetic energy of the different atoms by  $3k_B T/2$ , where  $k_B$  is Boltzmann's constant.

### 2.3. Radial distribution function analysis

Fourier transform of the reduced interference function  $Q_i(Q)$  gives the total pair correlation function

$$T(r) = 4\pi\rho_0 \left( \sum b_j \right)^2 + 2/\pi \int Q_i(Q)M(Q)\sin(Qr) dQ \quad (1)$$

where  $\rho_0$  is the total number density of atoms in the glass and  $M(Q)$  is the so-called modification function which downweights the termination ripples due to the finite experimentally measured  $Q$  range. In the present study,  $M(Q) = \sin(\alpha Q)/\alpha Q$  [28], was used with  $\alpha = 0.157$  for all samples.  $\alpha$  was determined from the condition  $M(Q_{\max} = 23 \text{ \AA}^{-1}) = 0.01$ . The statistical noise for the samples with  $x = 0.05$  and  $x = 0.10$  is slightly larger in this way but the corresponding  $T(r)$  functions can be compared using one and the same  $r$ -space resolution. All RDF calculations including the error analysis of the coordination numbers were performed with the program RADIF [29].

## 3. RESULTS AND DISCUSSION

The density of the glasses increases linearly for  $x > 0.05$  with increasing copper content (see Fig. 1) in accordance with the previous data for the  $\text{Cu}_x\text{As}_{0.50-x}\text{Te}_{0.50}$  series [3–6]. However, the comparison of the experimentally measured densities of the Cu-As-Te glasses with the density of As-Te binary alloys around the  $\text{As}_{0.5}\text{Te}_{0.5}$  composition,

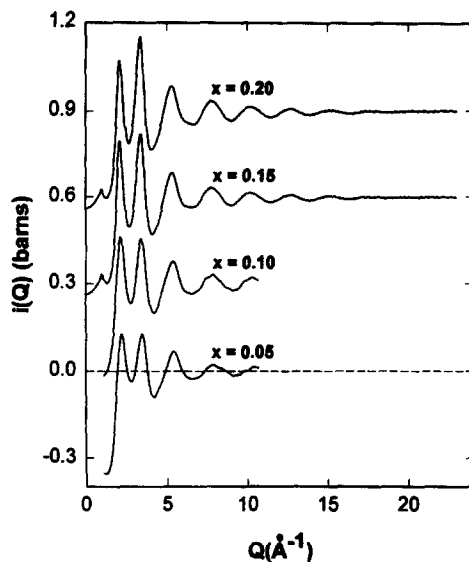


Fig. 2. Distinct scattering curves  $i(Q)$  for the investigated Cu-As-Te chalcogenide glasses. The curves for the glasses with  $x = 0.10, 0.15$  and  $0.20$  are shifted along the  $y$  axis by multiples of  $0.3$  barns for clarity.

$5.45 \pm 0.05 \text{ g/cm}^3$  [1, 17], indicates that there is a non-linear change of the compactness of the glasses going from low copper contents ( $x \leq 0.05$ ) to high copper content ( $x > 0.05$ ), while the glass transition temperature increases linearly in the whole compositional range studied.

The distinct scattering curves for the four samples, given in Fig. 2, are very similar in the range  $1.5\text{--}11 \text{ \AA}^{-1}$ , which is further evidence of the consistency of the data measured on different instruments. The curves for the samples with  $x = 0.15$  and  $x = 0.20$ , measured with high resolution in reciprocal space, show significant structural oscillations up to  $23 \text{ \AA}^{-1}$  and a weak but well defined FSDP at about  $0.98 \text{ \AA}^{-1}$ . The slope of the  $i(Q)$  curve at low  $Q$  for the sample with  $x = 0.05$  suggests that there is no FSDP in this composition but it was not possible to measure with this experimental setup  $i(Q)$  below  $1.08 \text{ \AA}^{-1}$ .

The corresponding total pair correlation functions  $T(r)$  are given in Fig. 3. The total pair correlation functions are very similar with 3 strong peaks at about  $2.61, 4.0$  and  $6.1 \text{ \AA}$ . The intensity of the  $6.1 \text{ \AA}$  peak and the additional structural correlations up to  $15 \text{ \AA}$  increases slightly with increasing  $x$ .

The position of the first RDF peak remains practically constant while the second and the third peaks shift linearly to higher  $r$  values with increasing copper content (Fig. 3). Evidently the structure expands and becomes more open with the addition of copper. The extrapolated value of the second  $T(r)$  peak at  $x = 0.0$ ,  $3.84 \pm 0.02 \text{ \AA}$ , is close to the distance  $3.9 \pm 0.03 \text{ \AA}$  observed in the As-Te binary alloys around the  $\text{As}_{0.5}\text{Te}_{0.5}$  composition [17, 19]. Comparison of the average nearest neighbour distances in several compositionally related crystalline and amorphous

Table 1. Average nearest neighbour distances in Cu-As-Te compounds

Bond	Bond length Å	Compound	References
Cu-Cu	2.63	CuTe	[30]
	2.70	Cu <sub>1.4</sub> Te	[31]
	2.64	Cu <sub>2</sub> As	[33]
Cu-As	2.55	Cu <sub>2</sub> As	[33]
Cu-Te	2.68	CuTe	[30]
	2.66	Cu <sub>1.4</sub> Te	[31]
As-As	2.44	c-As	[32]
As-Te	2.62	a-AsTe*	[17]
	2.78	As <sub>2</sub> Te <sub>3</sub>	[35]
Te-Te	2.83	Te	[36]

\* Amorphous As-Te alloy.

compounds [30–36] (see Table 1) indicates that all type of bonds between different atom pairs are possible in the range of the first  $T(r)$  peak between 2.2 and 3.1 Å. This fact accounts well for the observed compositional independence of the position of the first RDF peak and suggests that models with random bonding rather than with chemical short range ordering (CSRO) might describe better the structure of Cu-As-Te glasses.

The increase of the copper content leads to a systematic increase of the average coordination number, determined

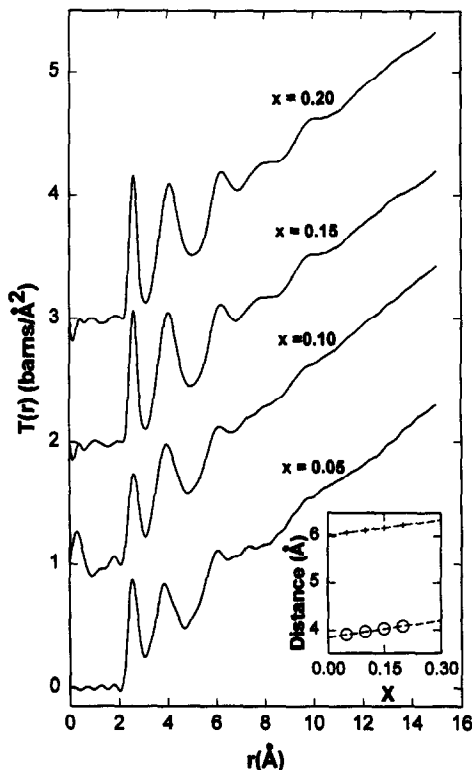


Fig. 3. Real space total correlation functions  $T(r)$  for the investigated  $\text{Cu}_x\text{As}_{0.45-x}\text{Te}_{0.55}$  chalcogenide glasses. The curves for the glasses with  $x = 0.10, 0.15$  and  $0.20$  are shifted along the y axis by multiples of  $1.0 \text{ barns}/\text{Å}^2$  for clarity. The inset shows the dependence of the position of the second ( $\circ$ ) and the third ( $+$ )  $T(r)$  peaks on composition. The dashed lines are linear fit through the data points.

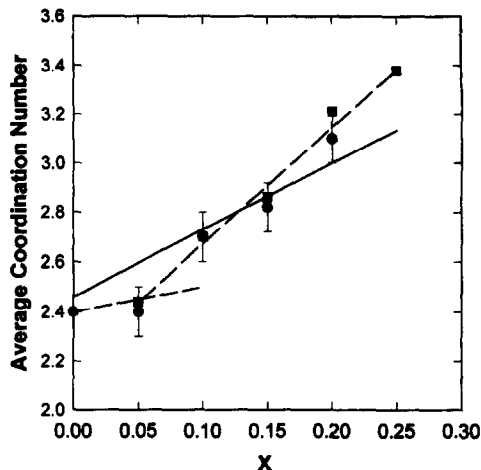


Fig. 4. Dependence of the average coordination number of Cu-As-Te chalcogenide glasses on the copper content  $x$ : ( $\circ$ )  $\text{Cu}_x\text{As}_{0.45-x}\text{Te}_{0.55}$ —present study, ( $\blacksquare$ )  $\text{Cu}_x\text{As}_{0.50-x}\text{Te}_{0.50}$  [3–6]. The full line is a fit to all data points of the equation  $2.45 + (1 + 0.55kx)$ , derived on the basis of the Formal Valence Shell model [37]. The dashed lines are calculated by eqns (2) and (3), respectively.

from the area under the first peak in the total radial distribution function  $rT(r)$  (Fig. 4). The average coordination numbers determined in the previous X-ray diffraction studies of several  $\text{Cu}_x\text{As}_{0.50-x}\text{Te}_{0.50}$  chalcogenide glasses [3–6] show a similar behaviour.

It is interesting to compare these results with the predictions of the Formal Valence Shell (FVS) model, proposed by Liu and Taylor [37] for multi-component chalcogenide glassy systems. According to the FVS model, based on the ideas of covalency and no doping, the copper should be four-coordinated. If we assume further, in the fashion of the FVS model, that: (i) As is three-fold coordinated; (ii) the coordination number of As does not change as Cu is added until all chalcogen atoms are fourfold coordinated [37]; and (iii) the coordination number of Te,  $n_{\text{Te}}$ , is two in the As-Te binary and increases linearly with the copper content ( $x$ ),  $n_{\text{Te}} = 2 + kx$ , then the average coordination number  $\langle \text{CN} \rangle$  can be written in the form  $\langle \text{CN} \rangle = 2.45 + (1 + 0.55k)x$ . We have fitted this equation to the experimentally determined coordination numbers, taking into account also the well established value  $\langle \text{CN} \rangle = 2.4 \pm 0.1$  for the As-Te binary composition. The fit, shown as a full line on Fig. 4 does not describe the data well and indicates that the mechanism of incorporation of copper in the As-Te binary glassy matrix depends on the composition. The simplest possible scenario can be the following.

At low copper contents the substitution of copper for arsenic practically does not change the Te coordination ( $k = 0$ ), so the average coordination number will be

$$\langle \text{CN} \rangle = 2.45 + x, \quad x < x_c \quad (2)$$

and only after some critical value,  $x_c$ , the average Te

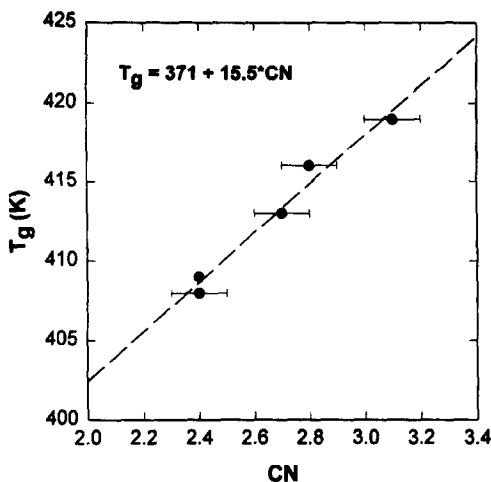


Fig. 5. Dependence of the glass transition temperatures  $T_g$  of the investigated  $\text{Cu}_x\text{As}_{0.45-x}\text{Te}_{0.55}$  chalcogenide glasses (●) on the average coordination number ( $\langle \text{CN} \rangle$ ). The dashed line is a regression curve with equation  $T_g(\text{K}) = 371 + 15.5\text{CN}$ .

coordination starts linearly to increase, so

$$\langle \text{CN} \rangle = (2.45 - 0.55kx_c) + 0.55kx, \quad x > x_c \quad (3)$$

A linear fit through the data at large  $x$  ( $x \geq 0.15$ ) was made using eqn (3) in order to determine the value of  $k$ . Equations (2) and (3) are shown with dashed lines on Fig. 4. From the intercept of the two lines we determined a critical composition  $x_c = 0.060 \pm 0.003$  which is not far away from the experimentally measured point at  $x = 0.05$ . Thus, the Te coordination increases from 2 at  $x = 0.06$  to 4 at  $x = 0.25$ .

Evidently,  $x_c = 0.06$  represents a cross-over point above which the addition of copper leads to more and more overconstraint network, in the sense of Phillips-Thorpe theory [38–40]. The increase of the rigidity of the glassy network suggests that the onset of viscous flow, commonly associated with the glass transition temperature  $T_g$ , must also increase. Considerable efforts have been made towards the understanding of the compositional dependence of  $T_g$  in chalcogenide glasses. In particular, several empirical expressions have been proposed, relating  $T_g$  to the average coordination number with different degree of success (for a review, see Ref. [41] and references therein). Plotting the experimentally determined  $T_g$  values for the investigated Cu-As-Te glasses versus the corresponding average coordination numbers, a clear correlation between  $T_g$  and  $\langle \text{CN} \rangle$  is observed (Fig. 5) with an equation

$$T_g(\text{K}) = 371 \pm 4 + 15.5 \pm 1.5 \langle \text{CN} \rangle \quad (4)$$

and a regression coefficient  $r = 0.9871$ . The correlation between  $T_g$  and  $\langle \text{CN} \rangle$  is in accordance with both the bond percolation and the free-volume models for the glass transition [42].

#### 4. CONCLUSIONS

The structure of several Cu-As-Te chalcogenide glasses with composition  $\text{Cu}_x\text{As}_{0.45-x}\text{Te}_{0.55}$ , where  $x = 0.05, 0.10, 0.15$  and  $0.20$ , has been examined by neutron diffraction. The structural results are correlated with density and glass transition temperature measurements. The high resolution state-of-the-art neutron diffraction measurements of the samples with high copper content ( $x = 0.15$  and  $0.20$ ) revealed for the first time the presence of a small but well defined first sharp diffraction peak (FSDP), not observed in previous X-ray diffraction experiments.

The analysis of the compositional dependence of the average coordination numbers in the framework of the Formal Valence Shell model [37] indicates that there is a critical composition  $x_c \approx 0.06$  below which the incorporation of copper does not lead to significant increase of the coordination number of chalcogen. Additional measurements of Cu-As-Te glasses with very low copper content ( $x < 0.05$ ) are in progress in order to confirm further these results. Above this critical composition the density and the average coordination number  $\langle \text{CN} \rangle$  increase linearly with increasing copper content. A correlation between the average coordination number and the glass transition temperature is also established which explains phenomenologically the observed increase of the onset of viscous flow.

*Acknowledgements*—N. Zotov acknowledges the financial support from the Spanish Interministerial Commission of Science and Technology. The additional beamtime allocated at the E2 diffractometer at BENSC, Berlin is highly appreciated.

#### REFERENCES

1. Borisova, Z. U., *Glassy Semiconductors*. Plenum Press, New York, 1981.
2. Dominguez, M., Vazquez, J., Villares, P. and Jimenez-Garay, R., *J. Phys. Chem. Solids*, 1991, **52**, 567.
3. Vazquez, J., Marquez, E., de la Rosa-Fox, N., Villares, P. and Jimenez-Garay, R., *J. Mater. Science*, 1988, **23**, 1709.
4. Wagner, Ch., Vazquez, P., Villares, P. and Jimenez-Garay, R., *Materials Letters*, 1993, **16**, 243.
5. Wagner, Ch., Vazquez, P., Villares, P. and Jimenez-Garay, R., *J. Mater. Science*, 1994, **29**, 3316.
6. Wagner, Ch., Vazquez, P., Villares, P. and Jimenez-Garay, R., *Il Nuovo Cimento*, 1994, **16**, 233.
7. Elliot, S.R., *Phys. Rev. Lett.*, 1991, **67**, 711.
8. Sokolov, A. P., Kisluk, A., Soltwisch, M. and Quitman, Q., *Phys. Rev. Lett.*, 1992, **69**, 1540.
9. Conejo, J. M., de la Rosa-Fox, N., Esquivias, L. and Jimenez-Garay, R., *Materials Letters*, 1986, **4**, 481.
10. de la Rosa-Fox, N. and Esquivias, L., *Mater. Sci. Letters*, 1988, **7**, 105.
11. Liang, K. S., Bienenstock, A. and Bates, C. W., *Phys. Rev. B*, 1974, **10**, 1528.
12. Gomez-Vela, D., Esquivias, L. and Prieto, C., *Phys. Status Solidi B*, 1992, **169**, 303.
13. Gomez-Vela, D., Esquivias, L. and Prieto, C., *Phys. Rev. B*, 1993, **48**, 10110.
14. Gomez-Vela, D., Esquivias, L. and Prieto, C., *J. Non-Cryst. Solids*, 1993, **167**, 59.

15. Saleh, Z. M., Williams, G. A. and Taylor, P. C., *J. Non-Cryst. Solids*, 1989, **114**, 58.
16. Benmore, C. J. and Salmon, P. S., *Phys. Rev. Lett.*, 1994, **73**, 264.
17. Comet, J. and Rossier, D., *J. Non-Cryst. Solids*, 1973, **12**, 61.
18. Faigel, Gy., Granasy, L., Vincze, I. and de Waard, H., *J. Non-Cryst. Solids*, 1983, **57**, 411.
19. Chang, J. and Dove, D. B., *J. Non-Cryst. Solids*, 1974, **16**, 72.
20. McGreevy, R. and Pusztai, L., *Mol. Simulations*, 1988, **1**, 359.
21. Hannon, A. C., Howells, W. S. and Sopper, A. K., *IOP Conf. Series*, 1990, **107**, 193.
22. Hohlwein, D., Hoser, A. and Prandl, W., *J. Appl. Cryst.*, 1986, **19**, 262.
23. Rietveld, H., *J. Appl. Cryst.*, 1969, **2**, 65.
24. Blech, I. A. and Averbach, B. L., *Phys. Rev. A*, 1965, **137**, 1113.
25. Paalman, H. H. and Pings, C. J., *J. Appl. Phys.*, 1962, **33**, 2635.
26. Sears, V. F., *Neutron News*, 1992, **3**, 26.
27. Johnson, P. A. V., Wright, A. C. and Sinclair, R. N., *J. Non-Cryst. Solids*, 1983, **58**, 109.
28. Lorch, E., *J. de Physique*, 1969, **C2**, 229.
29. Zotov, N., *Proceedings of the 11th National Conference, X-ray Diffraction Methods*, 20-22 May 1985, Primorsko, Bulgaria. Sofia University Press, 1985, pp. 132-139.
30. Anderko, K. and Schubert, K., *Z. Metallkunde*, 1954, **45**, 371.
31. Forman, S. A. and Peacock, M. A., *Am. Miner.*, 1949, **34**, 441.
32. Scheiferl, D. and Barret, C. S., *J. Appl. Cryst.*, 1969, **2**, 30.
33. Nand, J. and Priest, P., *Mat. Res. Bull.*, 1972, **7**, 783.
34. Carron, G. J., *Acta Cryst.*, 1963, **16**, 338.
35. Stergiou, A. G. and Rentzeperis, P. J., *Z. Kristallogr.*, 1985, **172**, 139.
36. Cherin, P. and Unger, P., *Act Cryst.*, 1967, **23**, 670.
37. Liu, J. Z. and Taylor, P. C., *J. Non-Cryst. Solids*, 1989, **114**, 25.
38. Phillips, J. C., *J. Non-Cryst. Solids*, 1979, **34**, 153.
39. Phillips, J. C. and Thorpe, M. F., *Solid State Commun.*, 1985, **53**, 699.
40. Thorpe, M. F., *J. Non-Cryst. Solids*, 1983, **57**, 355.
41. Tichy, L. and Ticha, H., *J. Non-Cryst. Solids*, 1995, **189**, 141.
42. Zallen, R., *The Physics of Amorphous Solids*. John Wiley and Sons, New York, 1983.